JCTC Journal of Chemical Theory and Computation

Article

pubs.acs.org/JCTC

Nonadiabatic Dynamics for Electrons at Second-Order: Real-Time TDDFT and OSCF2

Triet S. Nguyen and John Parkhill*

251 Nieuwland Science Hall, Notre Dame, Indiana 46556, United States

Supporting Information

ABSTRACT: We develop a new model to simulate nonradiative relaxation and dephasing by combining real-time Hartree−Fock and density functional theory (DFT) with our recent open-systems theory of electronic dynamics. The approach has some key advantages: it has been systematically derived and properly relaxes noninteracting electrons to a Fermi−Dirac distribution. This paper combines the new dissipation theory with an atomistic, all-electron quantum chemistry code and an atom-centered model of the thermal environment. The environment is represented nonempirically and is dependent on molecular structure in a nonlocal way. A production quality, $O(N^3)$ closed-shell implementation of our theory applicable to realistic molecular systems is presented, including timing information. This scaling implies that the added cost of our nonadiabatic relaxation model, time-dependent open self-consistent field at second order (OSCF2), is computationally inexpensive, relative to adiabatic propagation of real-time time-dependent Hartree−Fock (TDHF) or time-dependent density functional theory (TDDFT). Details of the implementation and numerical algorithm, including factorization and efficiency, are discussed. We demonstrate that OSCF2 approaches the stationary self-consistent field (SCF) ground state when the gap is large relative to k_bT. The code is used to calculate linear-response spectra including the effects of bath dynamics. Finally, we show how our theory of finite-temperature relaxation can be used to correct ground-state DFT calculations.

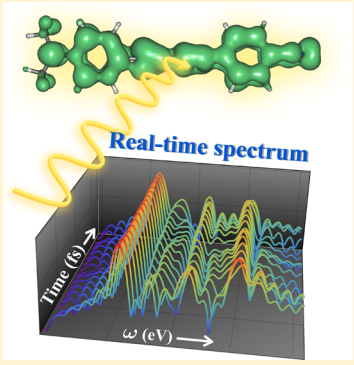

INTRODUCTION

To simulate realistic molecular absorption spectra and electronic dynamics, we must treat a combination of quantum degrees of freedom near zero temperature and thermal, nearly classical surroundings. However, the combination of quantum and classical degrees of freedom presents significant challenges to quantitative simulation. In this paper, we develop an atomistic model for the effects of thermalized surroundings on mean-field electronic dynamics produced by time-dependent density functional theory (TDDFT) and time-dependent Hartree−Fock (TDHF). The method is built on our self-consistent model for relaxation,[1] and so we call the combination with the mean-field electronic dynamics "time-dependent open self-consistent field at second order" (OSCF2). The computational cost scales cubically with the size of the system, rendering it affordable, relative to adiabatic time-dependent self-consistent field (TDSCF) calculations. The method is based on the one-particle density matrix and is free from the definition of any collective electronic state or many-electron wave function. Similar ideas are under active development in other research groups.[2−10]

Relative to other methods of nonadiabatic dynamics such as surface hopping,[11−14] *ab initio* multiple spawning,[15−17] and Ehrenfest dynamics,[18−20] OSCF2 has several important advantages. Most significantly, unlike any of the aforementioned models, this method naturally relaxes noninteracting electrons to a Fermi−Dirac (FD) distribution at long times. This is a critical condition which ensures that the dynamics reaches the correct end-point. OSCF2 also treats decoherence without any *ad hoc* assumptions. It has been systematically derived, allowing for straightforward incremental improvement and the incorporation of correlation effects in the theory. Moreover, the calculation of the bath model is inexpensive, relative to nonadiabatic dynamics that is based on collective electronic states. There are several limitations of OSCF2, relative to the common approaches for nonadiabatic dynamics. The main disadvantages stem from two assumptions: the Markov approximation and the choice of fixed bath model. Consequently, this theory is inappropriate for electronic dynamics that involve significant rearrangement of the nuclei, although this can be improved.

The paper is organized as follows: First, we will review the equation of motion (EOM) for the method, which includes the definition of an atom-centered bath. We will then discuss the computing cost and implementation. Finally, the behavior of several aspects of electronic dynamics will be examined: relaxation of particle-hole states and linear response spectra. We will also discuss the application of the method to correct *stationary* density functional theory (DFT) calculations at the dissociation limit.

Received: March 19, 2015

DOI: 10.1021/acs.jctc.5b00262
J. Chem. Theory Comput. XXXX, XXX, XXX−XXX

THEORY AND METHODS

Equation of Motion. The TDHF equations and time-dependent Kohn−Sham (KS) equations in the adiabatic approximation[21,22] can both be formulated as a Liouville-like nonlinear equation for the one-electron reduced density matrix (1-RDM, γ).[23] To propagate γ, we use real-valued single-particle bases: a set of nonorthogonal atom-centered functions (the AO-basis) labeled by Greek characters ($|\mu\rangle$, $|\nu\rangle$, ...), and an orthogonal basis of one-electron orbitals ($\phi_a(r)$, $\phi_b(r)$, ...). The occupation numbers of orbitals are unspecified and summation over repeated indices is implied. The molecular orbital coefficient matrix C defines the orthogonal functions in terms of the atomic functions: $C^a_\nu|\nu\rangle = |\phi_a\rangle$. The 1-RDM is the expectation value of a one-particle operator $\gamma^a_b = \langle a^a a_b\rangle$, where a^a and a_b are Fermion operators written in the notation of ref 24. Our code uses a singlet spin-adapted density matrix ($\gamma^a_b = \gamma^{a\alpha}_{b\alpha} + \gamma^{a\beta}_{b\beta}$). [Spin adaptation of the nonequilibrium part of our EOM is described in the Supporting Information.]

When $T = 0$, mean-field theory typically constrains the 1-RDM to be pure (idempotent, thus it satisfies $\gamma^2 = \gamma$). In this case, a single Slater determinant wave function corresponds to γ, and γ is a projector onto occupied orbitals. When the state is mixed because $T > 0$, the natural occupations (the eigenvalues of γ) are fractional ($\gamma^2 \neq \gamma$); the corresponding electronic state is no longer a single determinant. As long as the orbital occupations remain between zero and one, and sum to the number of electrons N,[25] the "1-positivity conditions", there is some valid state corresponding to the 1-RDM, although it usually is not a determinant. Consequently, it is simpler and clearer to describe the electronic state with the 1-RDM rather than the wave function when $T > 0$.

In an orthogonal basis, the Liouville-like equation of TDHF or TDDFT has the following form:

$$\dot{\gamma}(t) = \frac{-i}{\hbar}[\hat{F}\{\gamma(t)\}, \gamma(t)] \tag{1}$$

The Fock operator $\hat{F}$ is easiest to compute in the atomic basis, where it is $\hat{F}^\nu_\mu\{\gamma\} = \hat{h}^{\text{core}}_{\mu,\nu} + \sum_{\lambda,\sigma}\gamma_{\lambda,\sigma}[(\mu\nu|\sigma\lambda) - {}^1/_2(\mu\lambda|\sigma\nu)]$ for the TDHF method. This matrix can be transformed to the orthogonal basis $\hat{F}^a_b = C^a_\mu F^\mu_\nu C^b_\nu$. In TDDFT, the third term is replaced by an exchange correlation contribution.[26] If a time-dependent electric field $\vec{E}(t)$ is applied to the molecule, it adds a time-dependent perturbation to the Fock matrix:[27−31]

$$F^v_\mu(t) = F^v_\mu + \vec{E}(t)\cdot(\mu|\vec{r}|v)$$

Properties of the system, including the mean-field energy and dipole moment, are determined by γ.

With system-bath perturbation theory and Mukherjee and Kutzelnigg's extended normal ordering technique,[32] we have derived a Markovian dissipative correction to eq 1, which is also a functional of the 1-RDM, like TDHF:[1]

$$\dot{\gamma} = \frac{-i}{\hbar}[\hat{F}\{\gamma\}, \gamma] - \frac{1}{\hbar^2}\mathcal{R}\{\gamma\} \tag{2}$$

where

$$\begin{aligned}\mathcal{R}\{\gamma\}^a_b = \{&S_{a,f,f,c}\Gamma_\nu(\omega_{cf})V^\nu_{ae}V^\nu_{fc}\gamma^c_b\eta^e_f + S_{b,f,f,d}(\Gamma_\nu(\omega_{df})V^\nu_{be}V^\nu_{fd})^\dagger\gamma^a_d\eta^e_f \\ &- S_{d,b,a,c}\Gamma_\nu(\omega_{ca})V^\nu_{de}V^\nu_{ac}\gamma^c_d\eta^e_b - S_{c,a,b,d}(\Gamma_\nu(\omega_{db})V^\nu_{ce}V^\nu_{bd})^\dagger\gamma^c_d\eta^a_e\}\end{aligned} \tag{3}$$

and

$$S_{a,b,c,d} = \delta_{ab}\delta_{cd} + \delta_{bc}\delta_{ad}(1 - \delta_{ab}\delta_{cd}) \tag{4}$$

This term is dependent on a product of orbital coefficients, $V^\nu_{a,b} = \sum_\nu C^\nu_a C^{\nu\dagger}_b$, the one-hole density matrix $\eta^a_b = \delta^a_b - \gamma^a_b$, and a matrix of Markovian transition rates for each atomic function evaluated at the frequencies of orbital energy differences $\Gamma_\nu(\omega_{ab})$, where $\hbar\omega_{ab} = \epsilon_a - \epsilon_b$. We combine this dissipation theory with the KS density matrix, making the common approximation that this matrix represents the physical system[33] and that the nonadiabatic parts of the dissipation theory are negligible.[34,35] In the following section, we describe our model for Γ_ν and the bath. Code to propagate this nonlinear equation is described after that, followed by a comparison between theoretical and experimental benchmarks.

Markovian Rates. This work employs an atomistic version of a standard harmonic bath model, which supposes an environment can be modeled by an infinite number of noninteracting harmonic oscillators $\{\alpha\}$, bilinearly coupled with coupling constants $g_{\nu,\alpha}$ to the single-electron basis functions of a system. The density of environmental states, weighted by their coupling to a basis function μ, is a function called the spectral density (SD):

$$J_v(\omega) = \pi\sum_\alpha \hbar^2\omega_\alpha{}^2 g_{v,\alpha}{}^2\delta(\omega - \omega_\alpha)$$

In most open-systems theories, the SD is chosen to have a few, often arbitrary, parameters. Sometimes, parameters are chosen to loosely reflect the vibronic structure of the molecule.[36] However, detailed studies suggest that local variations in the SD are critical to dynamics.[37] We determine the SD with the fluctuations of the Fock matrix along an equilibrium molecular dynamics trajectory, by constructing the two-time correlation function $C_\mu(t) = \langle\hat{\Delta}_\mu(t)\hat{\Delta}_\mu(0)\rangle$ where $\Delta_\mu(t) = F_{\mu,\mu}(t) - \langle F_{\mu,\mu}\rangle$. The SD for electronic function μ then is given by the Fourier transform of $C_\mu(t)$ semiclassically.[38]

If we choose a numerical basis for $J_\mu(\omega)$, we would face numerical stability problems calculating dissipative rates as well as storage issues, since the SD is a heavily structured function with peaks at the molecule's vibrational resonances. Instead, we pursued a functional basis in which the dissipative rates can be calculated analytically, and which expresses the structure of $J_\mu(\omega)$ in compressed form, to avoid these issues. An important feature of our approach is a decomposition of the SD *for each atomic orbital* into a sum of as few Drude−Lorentz (DL) peaks as possible. Each peak is determined by its central frequency (Ω_i), its strength (λ_i), and its damping (γ_i). In terms of this DL basis, the system-bath coupling for each atomic orbital (μ) is unique and takes the following form:

$$J_\mu(\omega) = \sum_i \frac{\lambda_{\mu,i}}{\sqrt{\pi}}\left[\frac{\gamma_{\mu,i}}{\gamma_{\mu,i}{}^2 + (\omega - \Omega_{\mu,i})^2} + \frac{\gamma_{\mu,i}}{\gamma_{\mu,i}{}^2 + (\omega + \Omega_{\mu,i})^2}\right] \tag{5}$$

This basis of functions serves a role comparable to the Gaussian basis in an electronic structure code. It allows the dissipation to be calculated analytically, and since it is the response function of a damped harmonic oscillator, it is an efficient way to compress the infinite superposition of oscillators that comprise $J(\omega)$. However, like the Gaussian basis, it is nonorthogonal and overcomplete. We report the details of our procedure for assigning this basis elsewhere, and, in this work, we focus on the qualitative features of the dynamics.

Once a SD is known, Markovian rates are calculated as:

DOI: 10.1021/acs.jctc.5b00262
J. Chem. Theory Comput. XXXX, XXX, XXX−XXX

$$\Gamma_\nu(\omega_{ab}) = \int_0^\infty d\tau\, e^{i\omega_{ab}\tau} \times \left(\frac{1}{\pi}\right)\int_0^\infty d\omega' J_\nu(\omega')[e^{i\tau\omega'} n_b(\omega') + e^{-i\omega'\tau}(n_b(\omega') + 1)] \quad (6)$$

where n_b is the Bose−Einstein distribution. For a SD written as a linear combination of DL functions, this can be performed analytically. C++ code for the resulting expression is provided in the Supporting Information. It is critical that Γ_ν can be performed analytically, because there are $O(N^3)$ of these integrals to evaluate, and they must be updated when the Fock eigenvalues change significantly. We now discuss the efficient integration of the EOM.

Numerical Algorithm. The theory has been implemented for both TDHF and TDDFT in the Q-Chem quantum chemistry package[39] on top of existing ground-state complex-Hartree−Fock code.[40] The cost of building the Fock matrix can be as much as $O(N^3)$, and it is the bottleneck of a TDSCF calculation for most systems. We wanted OSCF2 to have the same range of applicability, so we pursued a fully factorized, vectorized, and multicore version of our dissipative theory. Remarkably, even though there are six indices in each term of the $\mathcal{R}$ expression, the CPU cost can be kept at $O(N^3)$ by properly introducing intermediates (Figure 1). For example, the

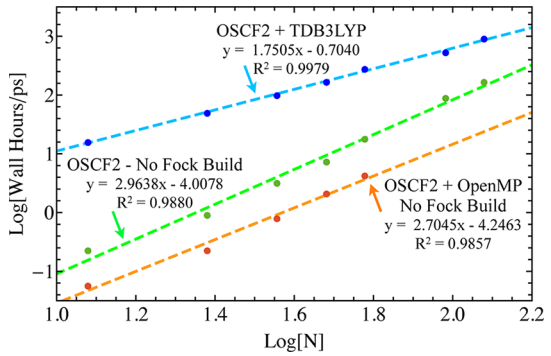

Figure 1. Timings (wall-hours per picosecond) and scaling of the code are demonstrated on a ring containing an increasing number of H atoms in the 6-311G** basis. Dashed lines are linear fit of sample points. The time step of propagation is held constant at 0.05 a.u., and the wall hours per picosecond are averaged over 1000 timesteps. When TDB3LYP is included, the Fock build is done at every time step. As can be seen from the slope of this plot, the dissipative portion of the code is genuinely $O(N^3)$, where N is the number of basis functions. The first example contains 12 basis functions, and the last 120 basis functions, which propagates $\mathcal{R}$ on one 2.1-GHz AMD piledriver core at a rate of 168 (h/ps).

last term involves two types of secular contributions, which are naively fourth-order:

$$S_{c,a,b,d}(\Gamma_\nu(\omega_{db})V^\nu_{ce}V^\nu_{bd})^\dagger\gamma^c_d\eta^a_e \rightarrow \sum_{\nu,a,c\neq e}(\Gamma_\nu(\omega_{ce})V^\nu_{ce}V^\nu_{ec})^\dagger\gamma^c_c\eta^a_e + \sum_{\nu,a,c,b}(\Gamma_\nu(0)V^\nu_{cc}V^\nu_{bb})^\dagger\gamma^c_b\eta^a_b \quad (7)$$

To evaluate the first of these terms in cubic time, we define $I_e = \sum_{\nu,c\neq e}(\Gamma_\nu(\omega_{ce})V^\nu_{ce}V^\nu_{ec})^\dagger\gamma^c_c$ and then multiply with η^a_e. Because there are twice as many factorized terms as nonfactorized terms, we omit the full mathematical expressions and instead include optimized code used to evaluate them in the Supporting Information. Every term is written as a combination of matrix multiplications, additions, and Schur products, which are vectorized. The optimized code has been checked against our initial naive implementation.

Modern electronic structure codes exploit basis set pair sparsity to reduce the cost scaling of a Fock build,[41,42] which our code does not. Even without this refinement, we can study realistic molecular systems in reasonable amounts of time (Figure 1). On a single node with multiple cores, a picosecond of dynamics for the benzene molecule in the 6-31G** basis can be propagated within a few hours with our code. The cost of evaluating the dissipative term with our implementation is inexpensive, relative to a Fock-matrix build for most molecules.

To integrate the EOM, an initial density is obtained from an ordinary SCF or linear-response calculation. The Fock matrix is then built and diagonalized, Markov rates are calculated, and the propagation begins. We use the Liouville-space split propagator technique[43] combined with the MMUT-TDHF method of Li et al.[44−46] (see Figure 2). Splitting the unitary and

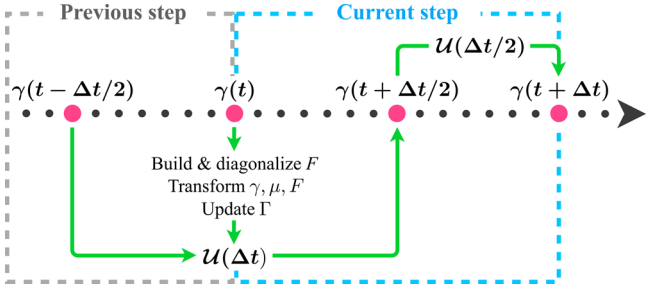

Figure 2. Modified MMUT scheme of one OSCF2 time step, given the propagator defined in eq 9.

dissipative parts of the propagation is advantageous. Dissipative terms cannot be integrated inexpensively by diagonalization, but they are energetically small and dynamically slow (>10 fs time scale), so even standard iterative methods such as Runge−Kutta are satisfactory. The unitary contributions to the propagator include core−valence energy differences, which are energetically large and dynamically fast (≪0.1 fs time scale), but can be inexpensively and accurately calculated treated after diagonalization. Other propagators, for example, those based on Krylov techniques or Magnus Expansion, may outperform this simple approach.

The MMUT technique for unitary TDHF discretizes the time-dependent and self-consistent changes in the Fock matrix at the center of a time step.[45] Our modification to MMUT simply replaces the unitary Fock propagator with a dissipative propagator for the density matrix $\mathcal{U}$. To derive $\mathcal{U}$, we separate the terms of eq 2 into its Fock contribution and dissipative contribution:

$$\dot\gamma(t) = \frac{-i}{\hbar}[\hat F\{\gamma\}, \gamma] - \frac{1}{\hbar^2}\mathcal{R}\{\gamma\} = \mathcal{L}\gamma = (\mathcal{L}_F + \mathcal{L}_R)\gamma(t) \quad (8)$$

Following Burghardt,[43] this equation can be solved as $\gamma(t+\Delta t) \approx \mathcal{U}(\Delta t)\gamma(t)$ by a split propagator of the form

$$\mathcal{U}(\Delta t) \approx \mathcal{U}_F\left(\frac{\Delta t}{2}\right)\mathcal{U}_R(\Delta t)\mathcal{U}_F\left(\frac{\Delta t}{2}\right) = e^{\mathcal{L}\Delta t} \approx e^{\mathcal{L}_F\Delta t/2}e^{\mathcal{L}_R\Delta t}e^{\mathcal{L}_F\Delta t/2} \quad (9)$$

The splitting is useful, because, in a canonical basis, the unitary (Fock) parts of this expression are trivial:

DOI: 10.1021/acs.jctc.5b00262
J. Chem. Theory Comput. XXXX, XXX, XXX−XXX

$$\gamma\left(t+\frac{\Delta t}{2}\right)_q^p = \mathcal{U}_F\left(\frac{\Delta t}{2}\right)\gamma(t) = \mathrm{e}^{-i\omega_{pq}\Delta t/2}\gamma_q^p$$

The dissipative part $\mathcal{U}_R(\Delta t)$ is approximated using a standard fourth-order Runge−Kutta equation:

$$\mathcal{U}_R(\Delta t)\gamma \approx \frac{\Delta t}{6}(k_1 + 2k_2 + 2k_3 + k_4) \tag{10}$$

where

$$k_1 = \mathcal{L}_R\gamma,\ k_2 = \mathcal{L}_R\left(\gamma + \frac{\Delta t}{2}k_1\right),\ k_3 = \mathcal{L}_R\left(\gamma + \frac{\Delta t}{2}k_2\right),$$
$$\text{and } k_4 = \mathcal{L}_R\left(\gamma + \frac{\Delta t}{2}k_3\right) \tag{11}$$

F is insensitive to the rapid oscillations of the coherences, and Γ_ν is relatively insensitive to the slow evolution of the orbital energies. To take advantage of this fact, F and Γ_ν can be optionally updated only when the norm of the change in orbital populations and energies exceeds 10^{-6}, respectively. Whenever F is rebuilt due to a change in density, all matrices including γ_q^p and V_{ab}^ν are transformed to the new eigenbasis. We have found that TDDFT propagation with OSCF2 is more sensitive to DFT quadrature grid accuracy than adiabatic theory. Propagation in this work uses Q-Chem's finest available quadrature grid. In all the following results, the trace of the density matrix was preserved within 10^{-5} electrons.

MODELS AND APPLICATIONS

Relaxation to Thermal Equilibrium. With a *fixed set of orbital energies*, we showed, in our previous work,[1] that OSCF2 reaches the exact FD populations at equilibrium. Now, combined with TDSCF, we would like to establish that the combined EOM properly equilibrates, and does not suffer from any type of nonlinear artifacts after a strong perturbation. For most spectroscopic applications, the k_bT value per gap is small and Fermi−Dirac populations are close to Aufbau populations; we show that OSCF2 equilibrates to an energy which matches ordinary ($T = 0$) mean-field theory within chemical accuracy.[47] In the later section, "Restricted Dissociation Curves and Thermalization", we show that, when the gap is on the order of k_bT, OSCF2's equilibrium state can actually improve on ($T = 0$) SCF calculations.

To study OSCF2 equilibration from a strongly perturbed initial condition, we perform a BLYP dynamics simulation after completely unfilling the HOMO and filling the LUMO. While the density relaxes, the orbital energies and rates of relaxation change significantly (Figure 3). The gap of this system is relatively large so the thermal electronic energy at 300 K is small, and we find OSCF2 approaches the ground-state energy well within chemical accuracy. The relaxation is exponentially slow; after 11 ps, the system is 62 μE_h above the ($T = 0$) ground-state energy. The relaxation does not have simple exponential or biexponential kinetics, but can be reasonably fit to two exponentials: $A\,\mathrm{e}^{-t/\tau_1} + (1 - A)\,\mathrm{e}^{-t/\tau_2}$, where $A = 0.87$, $\tau_1 = 7.65$ fs, and $\tau_2 = 86.95$ fs. The early, rapid rate corresponds to an unblocked HOMO orbital $\eta_{\mathrm{homo}} \approx 1$, and the later blocked rate to $\eta_{\mathrm{homo}} \approx 0$.

Visualization of Density Relaxation. In a typical weak-field excitation, less than a hundredth of an electron actually participates in dynamics. To visualize the density relaxation process following that excitation, we need to focus on the difference relative to the stationary state. Relaxation is otherwise hard to see behind all the other electrons. We have found the electron and hole density matrices are convenient for the purpose of visualizing dynamics. Head-Gordon et al. called this idea "attachment and detachment densities".[48] We determine the electron density as the sum of eigenvectors of the difference density with positive eigenvalues, and the hole density as the reverse. Note that the trace of the electron density is always the same as that of the hole density ($\int e(r,r)\,\mathrm{d}r = \int h(r,r)\,\mathrm{d}r$), since the total number of electrons is conserved. However, the trace of the electron and hole densities individually decay with time as the electronic system relaxes to the ground state, so that the difference density goes to zero and the ground state is found:

$$\delta\gamma(t) = \gamma(t) - \gamma_0;\ \ \lambda_{ii} = V_{ai}^\dagger \delta\gamma_b^a(t) V_{bi};\ \ e_b^a = \sum_{\lambda_i>0} V_{ai}\lambda_i V_{bi}^\dagger \tag{12}$$

In Figure 4, we show an example of a ring of H atoms whose electron density has been disturbed from the SCF stationary

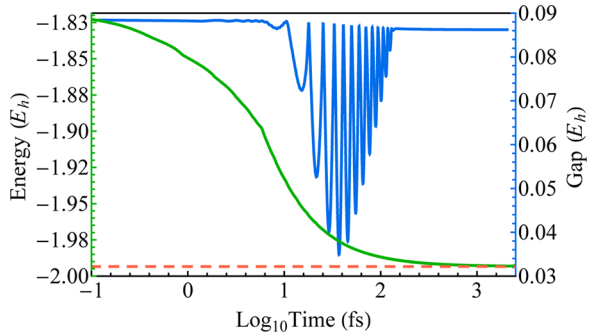

Figure 3. A 4 Å square of four H atoms (6-31G**, BLYP, 300 K) are propagated from a strongly perturbed particle−hole excitation. Note the $\log_{10}$(time) scale. On the right axis, the difference between the 2nd and 3rd orbital energy (blue) is plotted to show the relaxation of the Fock matrix. The electronic energy during relaxation (green) is plotted on the left axis. The red dotted line is at the ground-state energy ($-1.99339E_h$). Our dynamics reaches the ground-state energy and Aufbau populations of orbitals even though the Fock matrix changes significantly with time.

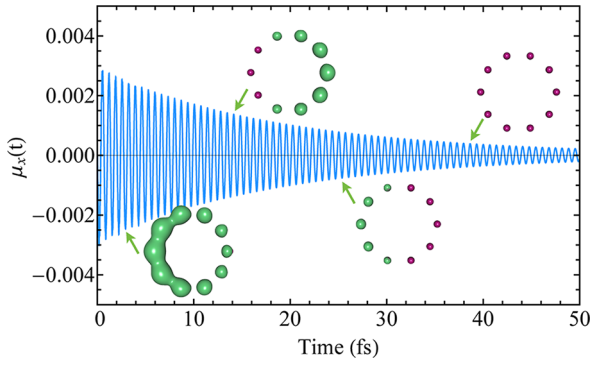

Figure 4. A 5 Å ring of 10 H atoms (6-31G**, B3LYP, 300 K) is subjected to a short electric field pulse in the x-direction, leading to a superposition of excited states with electron density that decays with time, because of the presence of the bath. The expectation value of the x-dipole moment are shown with the electron density. The electron density is shown at the same 5×10^{-6} electron contour, and it disappears as the total density returns to the ground state.

DOI: 10.1021/acs.jctc.5b00262
J. Chem. Theory Comput. XXXX, XXX, XXX−XXX

state due to a brief (0.07 a.u.) Gaussian electric field pulse of 0.001 a.u. in the x-direction. This results in a small oscillation of the density with snapshots for a given time over $\langle \mu_x(t) \rangle$. The electron density $e(r,r)$ shows the important dynamics very clearly, even though less than a thousandth of an electron is involved with the dynamics.

Linear Response Spectra. Real-time electronic dynamics codes can be used to produce isotropic linear absorption spectra by applying impulsive fields ($E(t) \propto \delta(t)$) along three axes of a molecule and Fourier transforming the resulting dipole oscillations (μ):[49]

$$\sigma(\omega) = \frac{4\pi\omega}{3c} \sum_{i=x,y,z} \frac{\mu_i(\omega)}{E_i(\omega)} \tag{13}$$

The "stick spectra" produced by adiabatic TDSCF (either real-time or linear-response) are sometimes difficult to correlate with broadened experimental spectra. This is partially because of geometric disorder but also the finite lifetime of states. Because density oscillations decay in our theory, the linear response spectra made by OSCF2 are naturally broadened. They also have a small Lamb shift from the imaginary part of $\mathcal{R}$. We can visualize the relaxation of individual excited states by performing a windowed Fourier transform of the dipole during relaxation.[50] As an example for large systems, we simulate the electronic dynamics of 1-cd, a diyne-bridged chromophore reported by Pati et al.[51] (see Figure 5). The environmental

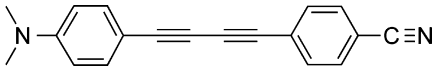

Figure 5. Structure of 1-cd (IUPAC name: 4-((4-(dimethylamino)-phenyl)buta-1,3-diyn-1-yl)benzonitrile).

effect is captured in an equilibrated dynamics simulation of one chromophore molecule in acetonitrile at 300 K. The solvent is modeled atomistically with the built-in QM/MM function of Q-Chem using the parameters of the CHARMM27 force field.[52,53] The resulting atomistic Drude-Lorentz SD is included in the Supporting Information. We calculate its real-time spectrogram from averaging a set of 10 geometries after excitation of a short (0.07 a.u.) Gaussian pulse of 0.001 a.u. in the x-direction (Figure 6a). This reveals the relaxation of the bright singlet at 2.95 eV and the more rapid relaxation of singlets from 3 eV to 7 eV over a very short time scale. In Figure 6b, the absorption spectrum calculated over the first 5 fs of dynamics shows the natural broad peaks of OSCF2 in good agreement with the experimental spectrum.[51] Note the Lamb shift of roughly 20 nm from the stick spectrum for the lowest-energy peak. We include, in the Supporting Information, a movie that shows rapid density oscillations of the chromophore within 2 fs after the impulse.

Redfield equations have constant relaxation rates $\mu(t) \propto e^{-\gamma t}$, and so they predict Lorentzian lineshapes. Relaxation rates in OSCF2 are not constant, because of Fermi blocking. The relaxation rate has a tendency to slow down over the course of dynamics, and so the line shape produced should not be purely Lorentzian. To examine the effect on predicted absorption line shape, we calculate the linear-response spectrum of the CO molecule[54] in the vicinity of an isolated transition two different ways: by Fourier transform of the dipole moment, and Lorentzian best-fit using the Harminv (Harmonic inversion) algorithm[55] (Figure 7). It appears that OSCF2's natural peakshape is essentially Lorentzian, despite the nonlinear changes in relaxation rate.

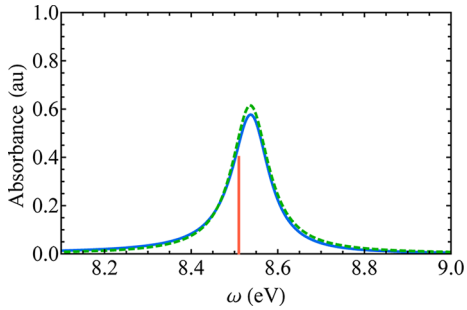

Figure 7. Linear-response spectrum of a CO molecule (B3LYP, 6-311G(2df,2pd)) generated by Fourier transform (blue solid) and Harmonic inversion (green dashed) shows the natural line shape of OSCF2 is almost exactly Lorentzian. The red line indicates the experimental position of the transition.

Restricted Dissociation Curves and Thermalization. Proper thermalization has important and even unexpected implications; one example is correcting the stationary electronic structure. Restricted Hartree−Fock theory fails when bonds are broken, because it cannot reach a qualitatively correct wave function. The correct density must half-occupy the HOMO and LUMO (which become degenerate at dissociation). Many (often costly) correlated methods have been developed to remedy this deficiency.[56−58] However, if orbitals are thermally populated,[59] the correct density is reached naturally at equilibrium, because the bath correctly adjusts the orbital occupation numbers and pushes electrons into the LUMO. This idea is the basis of the well-known Fermi-smearing method[60] for stabilizing SCF calculations on metals, and was

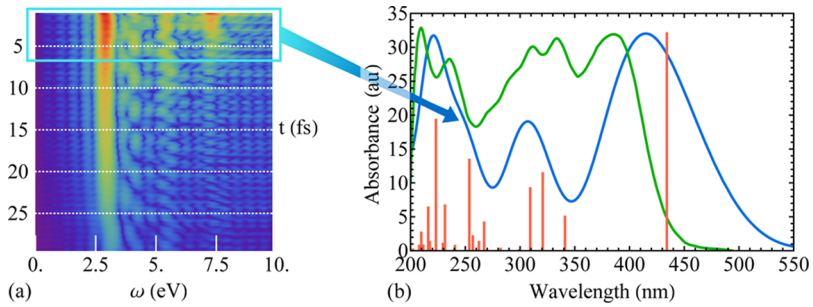

Figure 6. (a) Spectrogram of 1-cd generated from 30 fs dynamics. (b) The absorption spectrum (6-31G/B3LYP, blue), compared with the experimental absorption spectrum (green), and the linear-response stick spectrum (6-31G/B3LYP, red).

DOI: 10.1021/acs.jctc.5b00262
J. Chem. Theory Comput. XXXX, XXX, XXX−XXX

recently suggested as a correction to the KS method for molecules.[61] Because the orbital occupations of these methods are nonintegers, an entropy correction must be added to the mean-field energy, which has the following form, based on natural orbitals:[62]

$$G = E_{\mathrm{mf}} - TS = E_{\mathrm{mf}}\{\gamma\} - k_b T \sum_i \{\gamma_i \log(\gamma_i) + (\eta_i) \log(\eta_i)\} \quad (14)$$

Because our equation naturally reaches the correct thermal equilibrium, it also solves the restricted dissociation problem naturally. As an elementary example (Figure 8), we make a dissociation curve by propagating the normal restricted density of H_2 with a strong bath as close to stationarity as possible. We repeat this process for multiple internuclear separations. The bath naturally places the system in a mixed density, which has qualitatively correct dissociation behavior, despite remaining spin-pure.

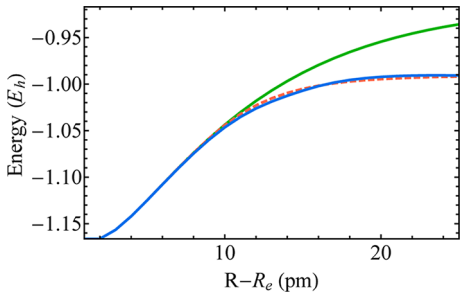

Figure 8. Stationary ground-state energies of restricted (green), unrestricted (red, dashed), and OSCF2 at $k_bT = 35.08E_h$ (blue) calculations of the H_2 molecule with the BLYP functional and 6-31G** basis set. OSCF2 dissociates to the correct unrestricted KS density, despite the fact that it is a restricted spin-pure theory. This is a natural consequence of the real thermalization physics in our model.

CONCLUSIONS

We have presented the implementation of our EOM, OSCF2, which is a nonequilibrium extension of the real-time SCF method, and applied it to the excited-state dynamics of molecular systems. The method can be used to study nonradiative relaxation and other interesting excited-state phenomena at a relatively low additional cost, compared to adiabatic DFT. We have examined the basic properties of the method and found that it equilibrates properly. Although relaxation rates are not constant with the method, it produces absorption lineshapes that are almost Lorentzian and match well with experimental spectra. We have also shown that the method can be used to study thermal electronic effects.

The theory we have presented can be used to study thermalization, relaxation, localization, quantum control,[63] and transport,[64] as well as linear and nonlinear spectroscopy.[65] Features that may be associated with long-lived electronic coherence in 2D nonlinear spectra are a topic of intense discussions.[66,67] However, because of the ambiguity of tight-binding theories for dissipation and absence of dephasing in ordinary electronic structure calculations, it has been difficult to separate electronic coherences from vibrational coherences. This work makes no assumption whatsoever of any discrete basis of states, and naturally treats decoherence, so it should be useful for clarifying these issues. The method is mainly limited by the accuracy of TDDFT and the assumption of a fixed bath model. In future work, we will use perturbation theory to treat correlation effects[68] in the dynamics, and improve the system-bath model. Integration of these models with affordable non-Markovian system bath approaches is also underway in our laboratory.

ASSOCIATED CONTENT

Supporting Information

Molecular geometry, spectral density, and density movie of chromophore 1-cd, and code fragments for Markovian dissipative correction and Markovian rates. The Supporting Information is available free of charge on the ACS Publications website at DOI: 10.1021/acs.jctc.5b00262.

AUTHOR INFORMATION

Corresponding Author

*E-mail: john.parkhill@nd.edu.

Notes

The authors declare no competing financial interest.

ACKNOWLEDGMENTS

We thank The University of Notre Dame's College of Science and Department of Chemistry and Biochemistry for generous start-up funding and Honeywell Corporation. T.S.N. gratefully acknowledges the support of the NSF Graduate Research Fellowship, under Grant No. DGE-1313583. We thank Sam Blau (Harvard) and Thomas Markovich (Harvard) for help with the Markovian rate expressions.

REFERENCES

(1) Nguyen, T. S.; Nanguneri, R.; Parkhill, J. *J. Chem. Phys.* **2015**, *142*, 134113.
(2) Yokojima, S.; Chen, G. H.; Xu, R. X.; Yan, Y. J. *Chem. Phys. Lett.* **2003**, *369*, 495−503.
(3) Goulielmakis, E.; Loh, Z.-H.; Wirth, A.; Santra, R.; Rohringer, N.; Yakovlev, V. S.; Zherebtsov, S.; Pfeifer, T.; Azzeer, A. M.; Kling, M. F.; Leone, S. R.; Krausz, F. *Nature* **2010**, *466*, 739−743.
(4) Kilin, D. S.; Micha, D. A. *J. Phys. Chem. Lett.* **2010**, *1*, 1073−1077.
(5) Zhang, Y.; Chen, S.; Chen, G. *Phys. Rev. B* **2013**, *87*, 085110.
(6) Koo, S. K.; Yam, C. Y.; Zheng, X.; Chen, G. *Phys. Status Solidi B* **2012**, *249*, 270−275.
(7) Ding, F.; Guidez, E. B.; Aikens, C. M.; Li, X. *J. Chem. Phys.* **2014**, *140*, 244705.
(8) Bjorgaard, J. A.; Kuzmenko, V.; Velizhanin, K. A.; Tretiak, S. *J. Chem. Phys.* **2015**, *142*, 044103.
(9) Head-Marsden, K.; Mazziotti, D. A. *J. Chem. Phys.* **2015**, *142*, 051102.
(10) Vogel, D. J.; Kilin, D. S. *Mol. Phys.* **2015**, *113*, 397−407.
(11) Tully, J. C. *J. Chem. Phys.* **2012**, *137*, 22A301.
(12) Lan, Z.; Fabiano, E.; Thiel, W. *J. Phys. Chem. B* **2009**, *113*, 3548−3555.
(13) Tapavicza, E.; Bellchambers, G. D.; Vincent, J. C.; Furche, F. *Phys. Chem. Chem. Phys.* **2013**, *15*, 18336−18348.
(14) Ouyang, W.; Dou, W.; Subotnik, J. E. *J. Chem. Phys.* **2015**, *142*, 084109.
(15) Ben-Nun, M.; Quenneville, J.; Martínez, T. J. *J. Phys. Chem. A* **2000**, *104*, 5161−5175.
(16) Levine, B. G.; Martínez, T. J. *J. Phys. Chem. A* **2009**, *113*, 12815−12824.
(17) Konar, A.; Shu, Y.; Lozovoy, V. V.; Jackson, J. E.; Levine, B. G.; Dantus, M. *J. Phys. Chem. A* **2014**, *118*, 11433−11450.
(18) Andrade, X.; Castro, A.; Zueco, D.; Alonso, J. L.; Echenique, P.; Falceto, F.; Rubio, Á *J. Chem. Theory Comput.* **2009**, *5*, 728−742.

(19) Liang, W.; Chapman, C. T.; Li, X. *J. Chem. Phys.* **2011**, *134*, 184102.
(20) Isborn, C. M.; Li, X.; Tully, J. C. *J. Chem. Phys.* **2007**, *126*, 134307.
(21) Furche, F.; Ahlrichs, R. *J. Chem. Phys.* **2002**, *117*, 7433−7447.
(22) Casida, M. E. *J. Mol. Struct.: THEOCHEM* **2009**, *914*, 3−18.
(23) McLachlan, A. D.; Ball, M. A. *Rev. Mod. Phys.* **1964**, *36*, 844−855.
(24) Kutzelnigg, W. *J. Chem. Phys.* **1982**, *77*, 3081−3097.
(25) Mazziotti, D. A. *Phys. Rev. Lett.* **2012**, *108*, 263002.
(26) Pople, J. A.; Gill, P. M.; Johnson, B. G. *Chem. Phys. Lett.* **1992**, *199*, 557−560.
(27) Li, X.; Smith, S. M.; Markevitch, A. N.; Romanov, D. A.; Levis, R. J.; Schlegel, H. B. *Phys. Chem. Chem. Phys.* **2005**, *7*, 233−239.
(28) Liang, W.; Chapman, C. T.; Li, X. *J. Chem. Phys.* **2011**, *134*, 184102.
(29) Chapman, C. T.; Liang, W.; Li, X. *J. Chem. Phys.* **2011**, *134*, 024118.
(30) Tapavicza, E.; Meyer, A. M.; Furche, F. *Phys. Chem. Chem. Phys.* **2011**, *13*, 20986−20998.
(31) Lopata, K.; Govind, N. *J. Chem. Theory Comput.* **2011**, *7*, 1344−1355.
(32) Kutzelnigg, W.; Shamasundar, K.; Mukherjee, D. *Mol. Phys.* **2010**, *108*, 433−451.
(33) Craig, C. F.; Duncan, W. R.; Prezhdo, O. V. *Phys. Rev. Lett.* **2005**, *95*, 163001.
(34) Tempel, D. G.; Aspuru-Guzik, A. *Chem. Phys.* **2011**, *391*, 130−142.
(35) Tempel, D. G.; Watson, M. A.; Olivares-Amaya, R.; Aspuru-Guzik, A. *J. Chem. Phys.* **2011**, *134*, 074116.
(36) Kumar, P.; Jang, S. *J. Chem. Phys.* **2013**, *138*, 135101.
(37) Renger, T.; Klinger, A.; Steinecker, F.; Schmidt am Busch, M.; Numata, J.; Müh, F. *J. Phys. Chem. B* **2012**, *116*, 14565−14580.
(38) Valleau, S.; Eisfeld, A.; Aspuru-Guzik, A. *J. Chem. Phys.* **2012**, *137*, 224103.
(39) Shao, Y.; Gan, Z.; Epifanovsky, E.; Gilbert, A. T.; Wormit, M.; Kussmann, J.; Lange, A. W.; Behn, A.; Deng, J.; Feng, X.; Ghosh, D.; Goldey, M.; Horn, P. R.; Jacobson, L. D.; Kaliman, I.; Khaliullin, R. Z.; Kuś, T.; Landau, A.; Liu, J.; Proynov, E. I.; Rhee, Y. M.; Richard, R. M.; Rohrdanz, M. A.; Steele, R. P.; Sundstrom, E. J.; Woodcock, H. L.; Zimmerman, P. M.; Zuev, D.; Albrecht, B.; Alguire, E.; Austin, B.; Beran, G. J. O.; Bernard, Y. A.; Berquist, E.; Brandhorst, K.; Bravaya, K. B.; Brown, S. T.; Casanova, D.; Chang, C.-M.; Chen, Y.; Chien, S. H.; Closser, K. D.; Crittenden, D. L.; Diedenhofen, M.; DiStasio, R. A.; Do, H.; Dutoi, A. D.; Edgar, R. G.; Fatehi, S.; Fusti-Molnar, L.; Ghysels, A.; Golubeva-Zadorozhnaya, A.; Gomes, J.; Hanson-Heine, M. W.; Harbach, P. H.; Hauser, A. W.; Hohenstein, E. G.; Holden, Z. C.; Jagau, T.-C.; Ji, H.; Kaduk, B.; Khistyaev, K.; Kim, J.; Kim, J.; King, R. A.; Klunzinger, P.; Kosenkov, D.; Kowalczyk, T.; Krauter, C. M.; Lao, K. U.; Laurent, A.; Lawler, K. V.; Levchenko, S. V.; Lin, C. Y.; Liu, F.; Livshits, E.; Lochan, R. C.; Luenser, A.; Manohar, P.; Manzer, S. F.; Mao, S.-P.; Mardirossian, N.; Marenich, A. V.; Maurer, S. A.; Mayhall, N. J.; Neuscamman, E.; Oana, C. M.; Olivares-Amaya, R.; O'Neill, D. P.; Parkhill, J. A.; Perrine, T. M.; Peverati, R.; Prociuk, A.; Rehn, D. R.; Rosta, E.; Russ, N. J.; Sharada, S. M.; Sharma, S.; Small, D. W.; Sodt, A.; Stein, T.; Stück, D.; Su, Y.-C.; Thom, A. J.; Tsuchimochi, T.; Vanovschi, V.; Vogt, L.; Vydrov, O.; Wang, T.; Watson, M. A.; Wenzel, J.; White, A.; Williams, C. F.; Yang, J.; Yeganeh, S.; Yost, S. R.; You, Z.-Q.; Zhang, I. Y.; Zhang, X.; Zhao, Y.; Brooks, B. R.; Chan, G. K.; Chipman, D. M.; Cramer, C. J.; Goddard, W. A.; Gordon, M. S.; Hehre, W. J.; Klamt, A.; Schaefer, H. F.; Schmidt, M. W.; Sherrill, C. D.; Truhlar, D. G.; Warshel, A.; Xu, X.; Aspuru-Guzik, A.; Baer, R.; Bell, A. T.; Besley, N. A.; Chai, J.-D.; Dreuw, A.; Dunietz, B. D.; Furlani, T. R.; Gwaltney, S. R.; Hsu, C.-P.; Jung, Y.; Kong, J.; Lambrecht, D. S.; Liang, W.; Ochsenfeld, C.; Rassolov, V. A.; Slipchenko, L. V.; Subotnik, J. E.; van Voorhis, T.; Herbert, J. M.; Krylov, A. I.; Gill, P. M.; Head-Gordon, M. *Mol. Phys.* **2015**, *113*, 184−215.
(40) Small, D. W.; Sundstrom, E. J.; Head-Gordon, M. *J. Chem. Phys.* **2015**, *142*, 024104.
(41) Cui, G.; Fang, W.; Yang, W. *Phys. Chem. Chem. Phys.* **2010**, *12*, 416−421.
(42) Schwegler, E.; Challacombe, M.; Head-Gordon, M. *J. Chem. Phys.* **1997**, *106*, 9708−9717.
(43) Burghardt, I. *J. Phys. Chem. A* **1998**, *102*, 4192−4206.
(44) Micha, D. A. *J. Phys. Chem. A* **1999**, *103*, 7562−7574.
(45) Li, X.; Tully, J. C.; Schlegel, H. B.; Frisch, M. J. *J. Chem. Phys.* **2005**, *123*, 084106.
(46) Castro, A.; Marques, M. A. L.; Rubio, A. *J. Chem. Phys.* **2004**, *121*, 3425−3433.
(47) Marzari, N.; Vanderbilt, D.; Payne, M. C. *Phys. Rev. Lett.* **1997**, *79*, 1337−1340.
(48) Head-Gordon, M.; Grana, A. M.; Maurice, D.; White, C. A. *J. Phys. Chem.* **1995**, *99*, 14261−14270.
(49) Tussupbayev, S.; Govind, N.; Lopata, K.; Cramer, C. J. *J. Chem. Theory Comput.* **2015**, *11*, 1102−1109.
(50) Akama, T.; Nakai, H. *J. Chem. Phys.* **2010**, *132*, 054104.
(51) Pati, A. K.; Mohapatra, M.; Ghosh, P.; Gharpure, S. J.; Mishra, A. K. *J. Phys. Chem. A* **2013**, *117*, 6548−6560.
(52) MacKerell, A. D.; Bashford, D.; Bellott, M.; Dunbrack, R. L.; Evanseck, J. D.; Field, M. J.; Fischer, S.; Gao, J.; Guo, H.; Ha, S.; Joseph-McCarthy, D.; Kuchnir, L.; Kuczera, K.; Lau, F. T. K.; Mattos, C.; Michnick, S.; Ngo, T.; Nguyen, D. T.; Prodhom, B.; Reiher, W. E.; Roux, B.; Schlenkrich, M.; Smith, J. C.; Stote, R.; Straub, J.; Watanabe, M.; Wiórkiewicz-Kuczera, J.; Yin, D.; Karplus, M. *J. Phys. Chem. B* **1998**, *102*, 3586−3616.
(53) Foloppe, N.; MacKerell, A. D., Jr. *J. Comput. Chem.* **2000**, *21*, 86−104.
(54) Chan, W.; Cooper, G.; Brion, C. *Chem. Phys.* **1993**, *170*, 123−138.
(55) Mandelshtam, V. A.; Taylor, H. S. *J. Chem. Phys.* **1997**, *107*, 6756−6769.
(56) Roos, B. O. *Advances in Chemical Physics*; John Wiley and Sons, Inc.: New York, 2007; pp399−445.
(57) Olivares-Amaya, R.; Hu, W.; Nakatani, N.; Sharma, S.; Yang, J.; Chan, G. K.-L. *J. Chem. Phys.* **2015**, *142*, 034102.
(58) Parkhill, J. A.; Lawler, K.; Head-Gordon, M. *J. Chem. Phys.* **2009**, *130*, 084101.
(59) Jacobi, S.; Baer, R. *J. Chem. Phys.* **2005**, *123*, 044112.
(60) Methfessel, M.; Paxton, A. T. *Phys. Rev. B* **1989**, *40*, 3616−3621.
(61) Chai, J.-D. *J. Chem. Phys.* **2012**, *136*, 154104.
(62) Ashcroft, N. W.; Mermin, N. D. *Solid State Physics*; Saunders College: Philadelphia, PA, 1976.
(63) Zhu, W.; Botina, J.; Rabitz, H. *J. Chem. Phys.* **1998**, *108*, 1953−1963.
(64) Uimonen, A.-M.; Khosravi, E.; Stefanucci, G.; Kurth, S.; van Leeuwen, R.; Gross, E. K. U. *J. Phys. Conf. Ser.* **2010**, *220*, 012018.
(65) Andrade, X.; Alberdi-Rodriguez, J.; Strubbe, D. A.; Oliveira, M. J. T.; Nogueira, F.; Castro, A.; Muguerza, J.; Arruabarrena, A.; Louie, S. G.; Aspuru-Guzik, A.; Rubio, A.; Marques, M. A. L. *J. Phys.: Condens. Matter* **2012**, *24*, 233202.
(66) Wong, C. Y.; Alvey, R. M.; Turner, D. B.; Wilk, K. E.; Bryant, D. A.; Curmi, P. M. G.; Silbey, R. J.; Scholes, G. D. *Nat. Chem.* **2012**, *4*, 396−404.
(67) Schlau-Cohen, G. S.; Ishizaki, A.; Calhoun, T. R.; Ginsberg, N. S.; Ballottari, M.; Bassi, R.; Fleming, G. R. *Nat. Chem.* **2012**, *4*, 389−395.
(68) Parkhill, J. A.; Markovich, T.; Tempel, D. G.; Aspuru-Guzik, A. *J. Chem. Phys.* **2012**, *137*, 22A547.

DOI: 10.1021/acs.jctc.5b00262
J. Chem. Theory Comput. XXXX, XXX, XXX−XXX